Brownian Motion of Nucleated Cell Envelopes Impedes Adhesion

Alexandra Zidovska* and Erich Sackmann

Physics Department E22, Technical University Munich, D-85748 Garching, Germany

(Received 4 August 2005; published 1 February 2006)

We demonstrate that composite envelopes of nucleated cells exhibit pronounced short wavelength (≤ 0.5 μm) bending excitations of ~ 10 nm root mean square amplitudes at physiological temperatures, which impede strong adhesion due to entropic repulsion forces. Quantitative microinterferometric analysis of the dynamic cell surface roughness of macrophages in terms of the theory of statistical surfaces suggests that the membrane excitations are mainly thermally driven Brownian motions (although active driving forces may contribute substantially). We determine the effective bending modulus of the cell envelope ($\sim 1000 k_B T$), the cortical tension ($\sim 10^{-4}$ N m^{-1}), and the work of adhesion ($\sim 10^{-5}$ J m^{-2}).

DOI: 10.1103/PhysRevLett.96.048103 PACS numbers: 87.68.+z, 83.60.−a, 87.16.−b, 87.17.−d

Introduction.—Numerous functions of cells such as adhesion, locomotion, and shape changes are determined by the adaptive mechanical properties of the composite cell envelope. This composite shell consists of a lipid-protein bilayer (the plasma membrane), which is locally anchored to a several hundred nanometer thick macromolecular network. A paradigm of these soft shells is the envelope of erythrocytes since its macromolecular scaffold consists of a very soft triangular network with the sides (~ 80 nm long) formed by flexible spectrin tetramers and the junctions (~ 35 nm long) by actin oligomers. The membrane associated scaffolds of nucleated cells (such as amoeboid Dictyostelia cells, endothelial cells, or white blood cells) are composed of semiflexible actin filaments that form a slightly cross-linked random network (mesh size $\uparrow 0.1$ μm, thickness $\uparrow 0.3$ μm [1]) if cells are kept in quiescent states [2]. A heterogeneous scaffold composed of a strongly cross-linked actin network coexisting with assemblies of actin bundles (acting as stress fibers) and actin-myosin assemblies (acting as micromuscles) forms if the cells are activated, e.g., by histamine [3]. Despite their complex structure, cell envelopes behave as perfectly elastic shells and show linear viscoelastic responses unless they are subjected to long time stresses (>30 sec) [3]. Erythrocyte shells are distinguished by their extreme softness with respect to shearing and bending and the absence of cortical tension. Their bending moduli are of the order of $10 k_B T$, and the shell exhibits pronounced bending excitations of ~ 100 nm amplitudes (often called flickering). They are thus often considered as biological manifestations of random surfaces [4,5]. Since the elastic moduli are smaller than expected for lipid bilayers containing ~ 50 mol % cholesterol ($\sim 100 k_B T$) and since Mg-ATPases are required to maintain the high softness, it was conjectured that the undulations are driven actively by chemomechanical forces [6,7]. The most intriguing and biologically important aspect of the cell surface roughness is that it generates strong entropic disjoining pressures [4,8]: $p_{\mathrm{disj}} \approx \frac{(k_B T)^2}{\kappa d^3}$ which surpass the van der Waals attraction at distances $d \leq 50$ nm and strongly weaken the specific receptor mediated attraction strength. It is often conjectured that undulation forces impede the adhesion of erythrocytes on the inner surfaces of blood vessels or of the spleen [9]. Undulation forces may, however, also drive the local attraction of receptors and conjugate ligands hidden within the glycocalix by inducing local phase separation of repeller molecules [10]. Up to the present it was assumed that thermally induced undulation forces do not play a role for normal cells, but are suppressed by strong cortical tensions generated by the coupling of the plasma membrane to the actin cortex and motor proteins myosin I [11]. In the present work we show for the first time quantitatively that white blood cells such as macrophages exhibit thermally driven surface roughnesses of the order of $\langle u^2 \rangle \sim 100$ nm^2, which suppress adhesion on glass. The shear elasticity does not suppress short wavelength excitation ($\Lambda \sim 1$ μm). The surface roughness coefficient $\langle u^2 \rangle$ increases by a factor of 5 after partial destruction of the actin cortex by the latrunculin. Flickering is suppressed by inhibition of myosin II activity by specific inhibitors of myosin light chain kinase after $t > 240$ min and the cells adhere strongly. Dynamic analysis of the contour of the surface of cells hovering over glass substrates by reflection interference contrast microscopy (RICM) allowed us to measure the surface roughness, the membrane tension, and the work of adhesion. The bending modulus of $\sim 1000 k_B T$ obtained by assuming that the dynamic surface roughness is determined by thermally excited bending undulations agrees well with values ($\sim 1000 k_B T$) measured for Dictyostelia cells [12] or quiescent endothelial cells. This allows us to apply models of statistical surfaces [4,13,14] to determine the persistence length of the roughness, the surface tension, the adhesion strength, and the second derivative of the cell-substrate interaction potential.

Cell preparations.—Mouse macrophages of strain J774 were cultivated in an incubator at 37 °C and 5% CO_2. The cell culture medium consisted of RPMI 1640 (Sigma, Germany) supplemented with 10% fetal bovine serum (Sigma, Germany) and 1% L-Glutamine (Sigma,

Germany). For each experiment cells were detached from the cell culture dish and transferred onto a cover glass. After incubating with cell culture medium for 24 h, the cover glass with sedimented cells and a Teflon frame forming the walls of the measuring chamber were assembled in a copper block, which was kept at 37 °C during all experiments.

Biochemical perturbations.—The state of the cells was modified by three types of biochemical agents: latrunculin, dimethylsulfoxide (DMSO), and PIK, a permeant specific inhibitor (PI) of myosin light chain kinase (MLC-Kinase). The sponge poison latrunculin binds strongly to monomeric actin and prevents the normal turnover of polymerized actin resulting in a transient partial decomposition of the actin cortex (cf. [3] for references). PIK was rendered membrane permeable by recombinant attachment of a precursor peptide (protein transduction domain). It inhibits very specifically MLC-Kinase [15]. It has been shown to lead to cell death within 240 min. DMSO is a nonspecific solvent that renders membranes permeable for solutes and could mediate the Ca influx into cells in a nonspecific manner.

Theory of statistical surfaces.—The dynamic roughness of composite cell envelopes is determined by all three modes of elastic deformation of shells: shearing, cortical tension, and bending elasticity. The mean square displacement of a mode of wave vector q can be expressed as

$$\langle u_q^2 \rangle L^2 = \frac{k_B T}{\kappa q^4 + \sigma q^2 + 2cq^3\sqrt{k_B T \mu} + \upsilon_2}. \quad (1)$$

c is a numerical factor: $c \approx 1.3$, κ, σ, and μ are the bending modulus, the lateral tension, and the surface shear modulus, respectively [4,5]. υ_2 is the curvature of a harmonic potential $\frac{1}{2}\upsilon_2(h - h_0)^2$ accounting for the interaction of the cell envelope with the solid surface, which suppresses long wavelength excitations [16]. The undulations are dominated by surface shear elasticity for wavelengths larger than

$$\Lambda_\mu = 2\pi q_\mu^{-1} = \frac{\pi\kappa}{c\sqrt{k_B T \mu}}. \quad (2)$$

The quiescent and weakly adhering macrophages are rather soft, and we can thus assume with some confidence that the surface shear elastic modulus is similar to that of endothelial cells for which $\mu \approx 10^{-4}\ \mathrm{N\,m^{-1}}$ was measured [3]. The effective bending modulus of composite cell envelopes (comprising the plasma membrane and the associated actin cortex) is expected to be of the order of $1000 k_B T$ (according to Ref. [12] and the discussion below), which yields a crossover wavelength of $\Lambda_\mu \approx 15\ \mu$m. This is much larger than the excitation wavelengths observed in our experiment ($\leq 1\ \mu$m), and we can thus neglect the contribution of shear elasticity.

Measurement of height fluctuations.—RICM images are formed by interference of the light reflected from the top surface of the substrate and the cell. The intensity distribution is thus the cosine transform of the time dependent height $h(x, y, t)$ of the cell over the substrate [18]:

$$\Delta i = \frac{2I(x, y, t) - (I_{\max} - I_{\min})}{I_{\max} - I_{\min}} = K \cos[2kh(x, y, t)], \quad (3)$$

where $I(x, y, t)$ is the measured intensity distribution of the image, $k = 2\pi n/\lambda$ is the wave vector of the incident light, and $K = (I_{\max} - I_{\min})/(I_{\max} + I_{\min})$ is the contrast where $I_{\max}$ and $I_{\min}$ are the maximum and minimum intensities of the interferogram, which can be determined from the intensity distribution of the interference fringes [6,18]. For our experiment, $\lambda = 546$ nm and $n = 1.34$, yielding $k = 15.4\ \mu\mathrm{m}^{-1}$.

The flicker amplitude was determined in two ways: first, by rigorous analysis of the normalized intensity distribution along linear sections through the RICM images [cf. Fig. 1(a)]. The mean square height fluctuations are obtained by subtracting the averaged height $2k\langle h(x)\rangle = \arccos\{\langle \Delta i(r, t)\rangle\}$ from the momentary profile $2k\{\langle h(x)\rangle + u(r, t)\} = \arccos\{\Delta i(r, t)\}$. The basis of the second procedure is that the flicker amplitudes are small compared to the average height $\langle h\rangle$ of the cell surface [6]. In this case the amplitudes can be directly obtained from the intensity difference $\delta\Delta i(r)$ [cf. Eq. (3)] according to [6]

$$\delta\Delta i(r) = k \sin\{k\langle h(r)\rangle\} u(r, t). \quad (4)$$

This procedure is best suited for the fluctuation analysis in the adhering area [19]. The absolute average height $\langle h(r)\rangle$ cannot be measured directly by RICM with one wavelength. The correction factor $\sin\{2k\langle h(r)\rangle\}$ is therefore determined by using the relation between the height of a statistical surface above a solid surface and the surface roughness $\langle u\rangle$, which can be expressed as $\langle h^2\rangle \approx 5\langle u^2\rangle$ [13].

Figure 1(a) shows a characteristic RICM micrograph of a cell showing the coexistence of adhering (dark area encircled by white line) and nonadhering regions (charac-

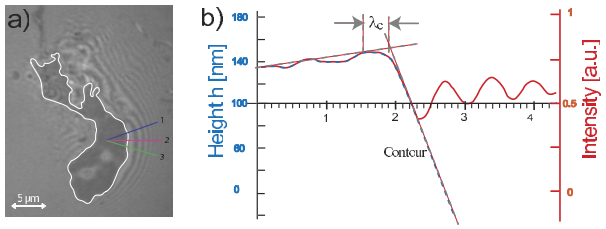

FIG. 1 (color online). (a) RICM micrograph of an adhering macrophage. The adhering area is marked by the white line. (b) The average intensity distribution $\langle \Delta i(r, t)\rangle$ is plotted on the right and the time averaged contour $\langle h(r, t)\rangle$ on the left ordinate scale (note that the scale for the average height holds only between $x = 0$ and 2.2 μm). The height difference between two maxima of the fringe pattern is given by $\Delta h_{\max,\max} = \lambda/2n \approx 546\ \mathrm{nm}/2.68 = 203.7\ \mathrm{nm}$ from which the contact angle Θ_c and the capillary length λ_c can be determined.

terized by a parallel fringe pattern). The fringes determine the lines of equal height $h_i(x, y)$ of the cell surface over the substrate. The average intensity and height distribution along the section AA' is presented in Fig. 1(b). The momentary intensity distributions $\Delta i(x, t)$ and heights $h(x, t)$ are measured along the sections every 87.71 nm at time intervals of 100 msec. Then the average intensity $\langle \Delta i(x, t) \rangle$, the intensity fluctuations $\delta \Delta i(x, t)$, and the undulation amplitudes $u(x, t)$ are determined as described above [20]. The dynamic roughness is obtained from the Gaussian distribution $P(u)$ of the amplitudes.

Evaluation of adhesion energy and membrane tension.—Direct inspection of the transient lateral displacements of the fringes shows that the excitation wavelengths are about 1 μm. By tentatively assuming that the undulations are determined by the bending elasticity (an assumption justified below) we can estimate the bending modulus from the roughness $\kappa = k_B T \xi_p^2 / 8\langle u^2 \rangle$. The value of $\kappa \approx 1000 k_B T$ obtained for $\langle u^2 \rangle \approx 30$ nm^2 and $\xi_p \approx 0.5$ μm [cf. Eq. (6)] is about equal to the bending modulus measured for quiescent Dictyostelia cells [12]. We can now determine the membrane tension and the work of adhesion by analyzing the contour of the contact zone in terms of elastic boundary conditions [21,22], which provide a relationship between the free energy of adhesion, W, and the cortical tension, σ (by the Young equation): $W = \sigma(1 - \cos\theta_c)$ and between W and the bending elastic modulus κ: $W = \kappa / 2R_c^2$, where θ_c is the contact angle [cf. Fig. 1(b)], R_c is the contact curvature at the transition between the adhering and nonadhering cell surface. R_c can be determined from the distance λ between the contact line and the point of intersection of the tangent to the nonadhering part of the cell surface with the surface [cf. Fig. 1(b)] according to $R_c = \lambda / \theta_c$ [22]. For the cell under physiological conditions we find $\tan\theta_c = 0.31$, $\sigma \approx 1 \times 10^{-4}$ N m^{-1}, and $W \approx 5 \times 10^{-6}$ J m^{-2} (cf. Table I). To judge the effect of the membrane tension, we consider now the relative flicker amplitudes expected for the above estimates of κ and σ and excitation wavelengths between $\Lambda = 0.3$ and 1 μm. The expected mean values of the amplitudes for the tension ($u_\sigma = 0.6$–2 nm) and for the bending dominated excitations ($u_\kappa = 0.2$–2 nm) are comparable, and the crossover from the bending to the tension dominated excitation regime occurs for wavelengths $\Lambda_{\sigma,\kappa} > 2\pi\sqrt{\kappa/\sigma} \approx 1.5$ μm. We thus conclude that the short wavelength (<1 μm) excitations studied in our experiments are not suppressed by the tension and are determined by the bending elastic excitations.

TABLE I. Summary of data obtained by assuming that the dynamic surface roughness is purely thermally driven and determined by bending elasticity. The bending modulus is determined by $\kappa / k_B T \sim \xi_p^2 / 8\langle u^2 \rangle$. The persistence length of the excitations is $\xi_p \approx 0.5$ μm. Note that κ is the effective bending modulus of the composite cell envelope.

	$\langle u \rangle$ (nm)	κ ($k_B T$)	λ (μm)	Θ_c (°)
Control cell	5.5 ± 1	1220	0.2	19
DMSO	7 ± 1	785	0.15	18
Latrunculin	11.0 ± 1	280	0.3	25

The above estimates strongly suggest that the dynamic surface roughness of the cell envelope is, indeed, mainly thermally driven, which allows us to analyze the data in terms of the statistical theory of adhering soft surfaces [4,5], based on the idea that the membrane is composed of cushions of lateral dimensions $\xi_p \times \xi_p$ that exhibit independent out-of-plane Brownian motions in the interaction potential imposed by the interfacial interaction with the membrane. The persistence length ξ_p is a measure for the distance over which a local bending excitation extends in the tangential direction. By approximating the interaction potential by a harmonic potential $V(h) = \frac{1}{2}\upsilon_2(h - \langle h \rangle)^2$ [cf. Equation (1)] or square well potential [13], one can determine various essential parameters characterizing the adhesion of the macrophages with solid surfaces. The absolute values of the average height $\langle h \rangle$ of the cell above the substrate can be obtained from the scaling law $\langle h \rangle^2 = c_s \langle u^2 \rangle$ [13], with $c_s = 5$ for weakly adhering membranes (cf. Table I). It is interesting to compare the result with the distance determined by the balance of the gravitational force of the cell $\Delta\rho g V$ and the entropic disjoining pressure:

$$g\Delta\rho V = A_c \frac{\delta V_H}{\delta h} = \frac{2 c_H A_c (k_B T)^2}{\kappa h^3}. \tag{5}$$

The numerical factor is $2c_H \sim 0.115$. For the density difference between cells and water $\Delta\rho \approx 125$ kg m^{-3}, a cell volume of $V = (4\pi/3)R^3 \approx 5 \times 10^{-16}$ m^3, and a contact area of $A_c \approx 25$ μm^2, one obtains $\langle h \rangle \approx 30$ nm, in reasonable agreement with the above estimation of $\langle h \rangle \approx 20$ nm based on the scaling law. The persistence length ξ_p and the second derivative of the interfacial interaction potential can be determined from the distribution of the mean square height fluctuations [10] [cf. Fig. 2(c)]:

$$P(h) = P_0 \exp\left[\frac{(h - \langle h \rangle)^2}{k_B T / \upsilon_2 \xi_p^2}\right] \tag{6}$$

by making use of the correlation between the roughness and the tangential persistence length $\xi_p^2 = (8\kappa / k_B T)\langle u^2 \rangle$. Inserting the data for the control cell, we obtain for the persistence length (or the diameter of the humps) $\xi_p \approx 0.5$ μm. With this value the curvature of the potential υ_2 is obtained from the width of the Gaussian height distribution ($\xi_p^2 \upsilon_2 = 2 \times 10^{-4}$ J m^{-2}) to $\upsilon_2 \approx 10^8$ J m^{-4}. This value is by a factor of 10 larger than the values found for weakly adhering giant vesicles ($\upsilon_2 \approx 10^7$ J m^{-4}).

Conclusions.—Nucleated cell envelopes with actin scaffolds can exhibit pronounced short wavelength bending excitations while long wavelength (>1 μm) modes are

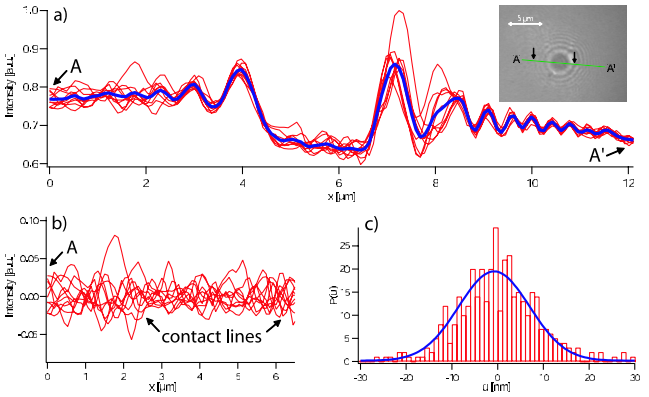

FIG. 2 (color online). (a) Plot of an average intensity distribution $\langle \Delta i(r,t) \rangle$ (thick line) and of momentary intensity distributions $\Delta i(x,t)$ along section AA' of the RICM image for a latrunculin treated cell. (b) Intensity fluctuations between A and the contact lines. Note that the fluctuation amplitude is of the same magnitude for both the adhering and nonadhering regions. (c) Example of a distribution of height fluctuations as a function of the root mean square displacements.

suppressed by the shear elasticity of the actin cortex. The bending modulus corresponding to thermal excitation ($\kappa \approx 1000 k_B T$) is comparable to the values found for quiescent nucleated cells. The reduction of κ by latrunculin by a factor of 5 is in agreement with results found for endothelial cells, but we do not find tether formation [23]. Our data suggest that the excitations are mainly thermally driven, although active forces may contribute (corresponding to a higher effective temperature [7]). An indication is the impediment of undulations by myosin II deactivation, which is, however, associated with stiffening of the actin cortex [3]. The excitation amplitudes are about equal to the length of headgroups of receptors ($\approx$ 15 nm for integrins), but are smaller than typical protrusion lengths of repeller molecules (40 nm). Thus, undulation driven collisions of cell envelopes with surfaces may promote receptor-ligand bond formation through repulsion of repellers from contact zones [10], and adhesion may be controlled by varying the disjoining pressure through the cortical tension.

This work was supported by the Bavaria California Technology Center (BaCaTeC), the Fonds der Chemischen Industrie, and the SFB 563. Helpful discussions with Robijn Bruinsma, Sam Safran, and Nir Gov are gratefully acknowledged.

*Corresponding author.
Present address: Materials Department, University of California, Santa Barbara, CA 93106, USA.
Electronic address: zidovska@mrl.ucsb.edu

[1] O. Medalia, I. Weber, S. Frangakis, D. Nicastro, G. Gerisch, and W. Baumeister, Science **298**, 1209 (2002).
[2] We denote freshly prepared cells exhibiting quasispherical shapes as quiescent cells. They exhibit isotropic and weakly cross-linked actin shells.
[3] W. Feneberg, M. Aepfelbacher, and E. Sackmann, Biophys. J. **87**, 1338 (2004).
[4] W. Helfrich, Z. Naturforsch. **33A**, 305 (1978).
[5] R. Lipowsky, *Generic Interaction of Flexible Membranes, Handbook of Biological Physics, Structure and Dynamics of Membranes* (Elsevier, Amsterdam, 1995), Vol. 1.
[6] A. Zilker, M. Ziegler, and E. Sackmann, Phys. Rev. A **46**, 7998 (1992).
[7] N. Gov, A. G. Zilman, and S. Safran, Phys. Rev. Lett. **90**, 228101 (2003); N. S. Gov and S. A. Safran, Biophys. J. **88**, 1859 (2004); S. Tuvia, S. Levin, A. Bitler, and R. Korenstein, J. Cell Biol. **141**, 1551 (1998).
[8] E. Evans, Langmuir **7**, 1900 (1991).
[9] K. Halder, B. Samuel, M. Narla, T. Harrison, and N. Hiller, Int. J. Parasitol. **31**, 1393 (2001).
[10] S. Marx, J. Schilling, E. Sackmann, and R. Bruinsma, Phys. Rev. Lett. **88**, 138102 (2002).
[11] J. Dai, J. P. Ting-Beall, R. M. Hochmuth, M. P. Sheetz, and M. A. Titus, Biophys. J. **77**, 1168 (1999).
[12] R. Simson, E. Wallraff, J. Faix, J. Niewohner, G. Gerisch, and E. Sackmann, Biophys. J. **74**, 514 (1998).
[13] R. R. Netz, Phys. Rev. E **51**, 2286 (1995).
[14] E. Frey and D. R. Nelson, J. Phys. I (France) **1**, 1715 (1991); D. R. Nelson and L. Peliti, J. Phys. (Paris) **48**, 1085 (1987).
[15] L. Shen, Y. Zolotarevsky, R. Mrsny, and J. Turner, BioConcepts **9**, 1 (2003).
[16] For wavelength of the order of the cell diameter one would have to consider spherical harmonic excitation and the coupling between bending and shearing [17], which would lead to a more complex expression. However, since the longest excitation wavelengths observed in our experiments are of the order of 1 μm, we can ignore this more rigorous theory.
[17] M. Peterson, Mol. Cryst. Liq. Cryst. **127**, 257 (1985).
[18] G. Wiegand, K. Neumaier, and E. Sackmann, Appl. Opt. **37**, 6892 (1998).
[19] The intensity distribution can be blurred by light reflected from intracellular structures. However, since their motions are slow compared to the bending excitations, these errors are averaged out. This assumption is justified by demonstrating that the amplitudes obtained by the two methods agree well.
[20] A. Zidovska, Diploma thesis, Technische Universitaet Muenchen, Germany, 2003.
[21] U. Seifert and R. Lipowsky, Phys. Rev. A **42**, 4768 (1990).
[22] Z. Guttenberg, B. Lorz, E. Sackmann, and A. Boulbitch, Europhys. Lett. **54**, 826 (2001).
[23] R. Bar-Ziv, T. Tlusty, E. Moses, S. A. Safran, and A. Bershadsky, Proc. Natl. Acad. Sci. U.S.A. **96**, 10 140 (1999).